Pure Appl. Geophys.

DOI 10.1007/s00024-014-0891-y

Pure and Applied Geophysics

Performance Benchmarking Tsunami Models for NTHMP's Inundation Mapping Activities

Juan Horrillo,[1] Stéphan T. Grilli,[2] Dmitry Nicolsky,[3] Volker Roeber,[4] and Joseph Zhang[5]

Abstract—The coastal states and territories of the United States (US) are vulnerable to devastating tsunamis from near-field or far-field coseismic and underwater/subaerial landslide sources. Following the catastrophic 2004 Indian Ocean tsunami, the National Tsunami Hazard Mitigation Program (NTHMP) accelerated the development of public safety products for the mitigation of these hazards. In response to this initiative, US coastal states and territories speeded up the process of developing/enhancing/adopting tsunami models that can be used for developing inundation maps and evacuation plans. One of NTHMP's requirements is that all operational and inundation-based numerical (O&I) models used for such purposes be properly validated against established standards to ensure the reliability of tsunami inundation maps as well as to achieve a basic level of consistency between parallel efforts. The validation of several O&I models was considered during a workshop held in 2011 at Texas A&M University (Galveston). This validation was performed based on the existing standard (OAR-PMEL-135), which provides a list of benchmark problems (BPs) covering various tsunami processes that models must meet to be deemed acceptable. Here, we summarize key approaches followed, results, and conclusions of the workshop. Eight distinct tsunami models were validated and cross-compared by using a subset of the BPs listed in the OAR-PMEL-135 standard. Of the several BPs available, only two based on laboratory experiments are detailed here for sake of brevity; since they are considered as sufficiently comprehensive. Average relative errors associated with expected parameters values such as maximum surface amplitude/runup are estimated. The level of agreement with the reference data, reasons for discrepancies between model results, and some of the limitations are discussed. In general, dispersive models were found to perform better than nondispersive models, but differences were relatively small, in part because the BPs mostly featured long waves, such as solitary waves. The largest error found (e.g., the laboratory experiment case of a solitary wave on a simple beach) was 10 % for non-breaking wave conditions and 12 % for breaking conditions; these errors are equal or smaller than the thresholds (10 % and 20 %, respectively) defined by the OAR-PMEL-135 for predicting the surface profile; hence, all models examined here are deemed acceptable for inundation mapping purposes.

Key words: Tsunami, tsunami numerical models, models comparison, models validation, dispersive models, nonhydrostatic models, hydrostatic models, NTHMP.

List of symbols

β	Slope angle (°)
$\overline{d}$	Physical channel depth (L)
η	Dimensionless free surface elevation (–)
η (cm)	Free surface elevation in centimeter (L)
$\overline{H}$	Physical incident wave height (L)
$\overline{g}$	Physical gravity acceleration (LT^{-2})
H	Dimensionless wave height (–)
R (cm)	Runup in centimeter (L)
t	Dimensionless time (–)
$\overline{t}$	Physical time (T)
t (s)	Time in seconds (T)
Xs	Incident wave initial position (L)
Xo	Slope toe location (L)
x	Horizontal coordinate system (L)
y	Vertical coordinate system (L)

1. Introduction

The coastal states and territories of the United States (US) are vulnerable to devastating tsunamis from near-field or far-field coseismic sources (e.g., American Samoa, the US Pacific west coast east of the Cascadia subduction zone, or Alaska) such as the 2004 Indian Ocean and 2011 Tohoku-oki events, Dunbar and Weaver (2008), and, also from less conventional sources, such as underwater and subaerial landslides (e.g., the upper US East Coast and Puerto Rico). In response to this threat, over the past

[1] Maritime Systems Engineering, Texas A&M University at Galveston, 200 Seawolf Pkwy, Galveston, TX 77554, USA. E-mail: horrillj@tamug.edu

[2] Department of Ocean Engineering, University of Rhode Island, Kingston, RI, USA.

[3] Geophysical Institute, University of Alaska Fairbanks, Fairbanks, AK, USA.

[4] Ocean and Resources Engineering, University of Hawaii, Manoa, HI, USA.

[5] Center for Coastal Resources Management, Virginia Institute of Marine Science, College of William and Mary, Williamsburg, VA, USA.

Published online: 25 July 2014

few decades, many of these states and territories have independently and gradually adopted or developed tsunami numerical models and carried out with those the development of tsunami inundation maps and community evacuation plans. In 2005, following the catastrophic 2004 Indian Ocean tsunami, this map development process was accelerated by the National Tsunami Hazard Mitigation Program (NTHMP). At the same time, NTHMP was mandated by the National Science and Technology Council to develop numerical model validation standards and coordinate tsunami hazard and risk assessment methodologies for all coastal regions of the US and its territories. The model validation standards were to be developed to ensure sufficient reliability of tsunami inundation maps, as well as a basic level of consistency between parallel state efforts, in terms of products. To satisfy this requirement, in 2011, a tsunami model validation workshop was held at Texas A&M University in Galveston. This workshop followed a model validation agenda based on the recommendations of Synolakis *et al.* (2007) (OAR-PMEL-135—tsunami model validation standard) to ensure that all tsunami numerical models be vetted through a standardized and identical process. The OAR-PMEL-135 report provides a list of tsunami benchmark problems (http://nctr.pmel.noaa.gov/benchmark/index.html) covering various tsunami processes. Depending on the type of benchmark (i.e., analytical, experimental, or historical), the report recommends different maximum error thresholds with respect to the reference data that tsunami model results must meet to be deemed acceptable. The operational and inundation-based (O&I) models ranged from models based on full three-dimensional (3-D) Navier–Stokes (NS) equations to two-dimensional (2-D) (depth-integrated) long wave models, with frequency dispersion (e.g., nonhydrostatic and Boussinesq models; BM) or without dispersion (nonlinear shallow water equations models; NSWE). As part of the workshop activities, each tsunami model was put through the same benchmarking process, depending on the "physics" featured in their equations or their intended use in the geographic area (e.g., coseismic sources) and results were compared between models and with the reference data. In this paper for sake of brevity, we only report in detail on two BPs based on laboratory experiments from the OAR-PMEL-135 report and present the cross-comparison between models and reference data. It should be noted that not all tsunami models were applied to the selected BPs, i.e., the 3-D NS models are not included in the model cross-comparison due to their intended use in the geographic area, e.g., landslide sources, which is not the purpose of these two selected BPs. However, detailed characteristics, capabilities, and testing procedures, for these 3-D NS models and also for those intended for coseismic sources are fully documented in the workshop proceedings, NTHMP (2012) (http://nthmp.tsunami.gov/publications.html).

2. A Review of Tsunami Numerical Models

Over the past few decades, a variety of tsunami generation and propagation models have been developed, based on different classes of governing equations, numerical methods, spatial and temporal discretization techniques, and wetting-drying algorithms used to predict tsunami runup. Among these, the vast majority of the current O&I tsunami models are based on depth-integrated, hydrostatic or nonhydrostatic long wave equations. A brief review of the main classes of O&I tsunami models follows.

Long wave models solving linear shallow water wave equations (LSWEs) were initially developed based on finite difference methods (FDMs), following the work of Hansen Hansen (1956) and Fischer (1959). A detailed review of these models can be found in Kowalik and Murty (1993) and Imamura (1996). On the basis of these initial FDM approaches, in the early 1990s, the tsunami propagation model referred to as TUNAMI (Tohoku University's numerical analysis model for investigation; Imamura *et al.* 1995) was developed based on nonlinear shallow water equations (NSWEs). In this model, the kinematics of surface elevation near the shoreline is computed by parameterizing a water flux quantity, the so-called "discharge" Imamura (1996), and the NSWEs are formulated in a flux-conservative form, which enforces mass conservation throughout computations. The ALASKA-tectonic (GI′-T) and -landslide (GI′-L) models follow an almost identical approach, i.e., a staggered leapfrog FDM scheme is

used to solve NSWEs formulated for depth-averaged water fluxes on a Arakawa C-grid layout Kowalik and Murty (1993), Arakawa and Lamb (1977). A recent and extensive discussion of these models can be found in Nicolsky *et al.* (2011). A similar numerical model, also extensively used for operational tsunami modeling, is the method of splitting tsunami (MOST, Titov and Synolakis 1995), which can compute tsunami propagation by using a variable space grid or free parameters (numerical dispersion, Burwell *et al.* 2007) in a manner that allows mimicking theoretical dispersion and extending its capability to simulate weakly dispersive tsunamis. An innovative approach in MOST is its ability to track the shoreline by adding new grid points as a function of time. As mentioned, the MOST model is used in operational (real-time) forecasting; examples of the model's forecasting capability are given in Wei *et al.* (2008) and Tang *et al.* (2012). GeoClaw is another recent tsunami model, also based on the NSWE approximation, which offers a unique solution to the problem associated with transferring fluid kinematic throughout nested grids Berger and LeVeque (1998). To do so, GeoClaw uses a dynamic mesh refinement for an arbitrary number of nested levels. As the calculation progresses, individual grid cells are tagged for refinement, using a criterion such as wave height or by directly specifying the region of interest; thus, disturbed water parcels or those in specified regions are gradually better resolved. The flagged cells at each level are clustered into rectangular patches, for refinement to the next level, as described in detail in Berger and LeVeque (1998).

NSWE models assume a hydrostatic pressure and, hence, are nondispersive, which limits their range of applicability to studying very long waves. However, tsunamis caused by smaller size seabed failures (such as underwater landslides or splay faults) are made of shorter wave trains for which frequency dispersion becomes important. Similarly, long tsunami waves propagating over wide shallow shelves often develop highly dispersive undular bores near each long wave crest Grilli *et al.* (2013). To allow for such more extended physics, since the late 1990s, models based on depth-integrated Boussinesq equations have been applied to simulate tsunami propagation. While the original Boussinesq equations were only weakly nonlinear and dispersive Peregrine (1967), fully nonlinear approximations with extended dispersion properties were developed (e.g., Nwogu 1993; Wei *et al.* 1995; Kirby *et al.* 1998; Lynett *et al.* 2002). In shallow water, these so-called fully nonlinear Boussinesq models (FNBMs) extend NSWEs to include nonhydrostatic/dispersive effects. FNBMs, which are typically more computationally demanding than NSWE models, are now very efficiently implemented on large parallel clusters, using nested grid algorithms (e.g., FUNWAVE-TVD; Shi *et al.* 2012), making it possible to simulate some of the recent significant tsunami events using large finely refined grids (e.g., Watts *et al.* 2003; Ioualalen *et al.* 2007; Tappin *et al.* 2008; Grilli *et al.* 2010, 2012). FUNWAVE-TVD includes all the important features necessary for tsunami prediction, such as moving shoreline for runup, bottom friction, energy dissipation to account for wave breaking, and a subgrid turbulence scheme. Another FNBM capable of simulating accurate near-field tsunami scenarios is BOSZ (Boussinesq Model for Ocean and Surf Zones; Roeber and Cheung 2012). The model combines the weakly dispersive properties of the Boussinesq approximation with the shock capturing capabilities of the conservative form of the NSWEs Nwogu (1993) up to fifth-order on Cartesian coordinates. The model is primarily used to simulate nearshore wave processes (e.g., modeling surf zone and swash processes of swell and wind waves) but is well suited for numerical simulations of wave propagation over shallow fringing reefs.

Other governing equations for modeling dispersive waves have been proposed by Stelling and Zijlema (2003), which include a nonhydrostatic pressure gradient in a multiple layer solution of NS equations which provides dispersive properties comparable to those of extended FNBMs. A tsunami propagation model based on this approach is the nonhydrostatic evolution of Ocean WAVEs (NEOWAVE) Kowalik *et al.* (2005), Yamazaki *et al.* (2009), in which the nonhydrostatic pressure and the vertically averaged velocity resulting from the related kinematic boundary condition at the free surface and on the seafloor are implicitly computed. This model was successfully applied to recent tsunami case studies (e.g., Yamazaki *et al.* 2011a, b). A similar

nonhydrostatic NSWE model, currently used for operational tsunami forecasting in the West Coast and Alaska Tsunami Warning Center, is the Alaska Tsunami Forecast Model (ATFM) Kowalik and Whitmore (1991), Whitmore and Sokolowski (1996), which uses structured nested meshes defined as a function of water depth (isobaths) and bathymetric resolution. Surface elevation is computed based on mass conservation, using a second-order upwind scheme van Leer (1977), and run-up/run-down at shorelines are computed with a volume of fluid (VOF) approach Nichols *et al.* (1980), Hirt and Nichols (1981). Another non-hydrostatic, and well-known community supported model is the semi-implicit Eulerian–Lagrangian finite elements (SELFE, Zhang and Baptista 2008), which are based on the 3-D NS equations and usean unstructured grid in the horizontal dimension to allow fitting complex coastal topographic features as well as coastal structures. The model can be configured in multiple ways (e.g., hydrostatic or nonhydrostatic), but in tsunami applications the 2-D depth-averaged hydrostatic configuration is typically used for maximum efficiency.

Nonhydrostatic and Boussinesq depth-integrated models perform extremely well for most tsunami scenarios but may not satisfactorily work for cases where simulating the full 3-D fluid flow structure is important, such as in landslide tsunami generation. In their active wave generation region, landside tsunamis are more accurately simulated using either 2-D + 1-D (horizontal × vertical) or fully 3-D NS models (e.g., Abadie *et al.* 2010; Horrillo *et al.* 2010; Ma *et al.* 2012), which if required can also account for multiple fluids (e.g., air, water) and materials (e.g., debris flow or rock slide). One of the earliest numerical models of this type was developed by Harlow and Welch (1965) and then further extended to full 3-D based on the work of Nichols and Hirt (1975) and Rider and Kothe (1995). While even today the use of a 3-D NS solver is still computationally prohibitive in typical tsunami domains that cover large spatial areas (e.g., transoceanic dispersive wave propagation), efficient-parallelized 3-D NS models have been applied to smaller spatial areas, such as for computing landslide or subaerial tsunami source generation, or tsunami inundation regions, where more accuracy on vertical fluid acceleration or runup are needed. In practical tsunami simulations involving landside tsunami or complex coseismic thrust, a typical approach is to use a hybrid model in which the 3-D NS model is used for simulating the tsunami generation phase (i.e., the tsunami source), and its 3-D solution at a predetermined time is reinterpolated onto a more efficient 2-D Boussinesq or nonhydrostatic model for further simulating the propagation and the inundation phases. Models that have recently used this approach for simulating historical case studies and developing tsunami inundation maps are TSUNAMI3D Horrillo *et al.* (2010, 2013) and THETIS Abadie *et al.* (2012), Harris *et al.* (2012). These models solve transient incompressible fluid flows with free surface and interfacial boundaries described based on the concept of the fractional VOF. These models were also validated for analytical and experimental benchmark cases, and details of their results can be found in the workshop proceedings, NTHMP (2012).

Table 1 summarizes the main features of the tsunami models that were benchmarked and compared in the workshop and in this paper.

3. Benchmark Problems

The initial set of BPs was assembled based on the recommendations of OAR-PMEL-135's report Synolakis *et al.* (2007, see also 2008), which originated in past tsunami model validation workshops organized to verify the performance of tsunami models according to the state of knowledge and data obtained from historical tsunamis at the time. These were the 1995 Long-Wave Run-up Models Workshop held in Friday Harbor, Washington and the 2004 Workshop held in Catalina Island, California. The report gives a brief description of each BP and their intended purpose, with the complete data being available at http://nctr.pmel.noaa.gov/benchmark/. The NTHMP requires that all tsunami inundation-based models used in inundation mapping be validated and verified; additionally, although not mandatory, it is desirable that operational models used in tsunami warning or emergency planning be similarly validated (e.g., tsunami forecasting models). According to these

Table 1

Summary of model characteristics

Model/features	ALASKA	ATFM	BOSZ	FUNWAVE	GeoClaw	MOST	NEOWAVE	SELFE	THETIS	TSUNAMI3D
Approximation	NSWE	Hyd/non-hyd	FNBM	FNBM	NSWE	NSWE	Hyd/non-hyd	Hyd/non-hyd	3-D NS	3-D NS
Wave dispersion	No	Yes (optional)	Yes	Yes	No	No	Yes	Yes (optional)	Yes	Yes (optional)
Grid nesting	Two-way	Two-way (submeshes)	No	One-way	Two-way (Adaptive mesh refinement)	One-way	Two-way	Two-way unstructured mesh	Structured variable mesh	Structured variable mesh
Coordinate system	Cartesian/ spherical	Cartesian/ spherical	Cartesian	Cartesian/ spherical	Cartesian/ spherical	Cartesian/ spherical	Cartesian/ spherical	Cartesian/ spherical	Cartesian/ cylindrical	Cartesian
Numerical scheme	Finite difference	Finite difference	Finite volume	Finite difference/ finite volume	Finite volume	Finite difference	Finite difference	Finite element/ finite volume	Finite volume	Finite volume
Tsunami source	Coseismic + landslide	Coseismic	Coseismic	Coseismic + landslide (initializ. THETIS)	Coseismic + landslide	Coseismic	Coseismic + landslide (initializ. TSUNAMI3D)	Coseismic	Landslide (coupled to FUNWAVE)	Landslide (coupled to NEOWAVE)
Run-up approach	Moving boundary	Volume of fluid	Shock-capturing/ Riemann solution	Slot technique	Shock-capturing/ Riemann solution	Horizontal projection	Horizontal projection	Iterative projection	Volume of fluid	Volume of fluid
Parallelization	MPI	Co-array	OpenMP	MPI	OpenMP	OpenMP	No	MPI	MPI	OpenMP/MPI
Documentation	Limited	Limited	Limited	Yes	Yes	Limited	Yes	Yes	Yes	Limited
Execution	Graphics interface	Command line	Command line/ graphics interface	Command line	Command line	Graphics interface	Command line	Command line	Command line	Command line

Table 2

Allowable errors for the three categories used for benchmarking

Category	Allowable errors Wave amplitude/runup
Analytical solution	<5 %
Laboratory experiment	<10 %[†]
Field measurments	<20 %

[†] Laboratory experiments involving breaking waves the allowable error is <20 %

requirements, all O&I models must be validated against analytical, experimental, or field BPs that cover the range of planned applications of each particular model. In this paper for sake of brevity, only two laboratory experimental BPs are presented for the cross-comparison between models. Allowable error thresholds are used to decide whether a model has adequately simulated the selected BPs; specifically, these are 5, 10 and 20 % average relative error on model parameters (e.g., maximum surface amplitude/run-up) or/and the normalized root mean square desviation error (e.g., water surface snapshoot or time series) with respect to the reference data, for three categories of analytical, laboratory, and field BPs, respectively, see NTHMP (2012). The specified error of <10 % for laboratory experiments is replaced by <20 % for challenging laboratory experiments, such as those involving breaking waves (see Table 2).

In this paper, the selected subset of BPs for the cross-model comparison both fall within the laboratory experiment category and are described in great detail in the OAR-PMEL-135 report listed as: (a) solitary wave on a simple beach and (b) solitary wave on a conical island. However, we give a brief description of these two selected laboratory experiments below.

3.1. Laboratory Experiment: Solitary Wave on a Simple Beach

This test depicted and referenced to as BP4 in NTHMP (2012), is based on a laboratory experiment carried out in a 32 m long wave tank at the California Institute of Technology. The geometry of the tank and laboratory equipment used to generate long waves are described in detail by Hammack (1972), Goring (1978) and Synolakis (1986). The bathymetry consists of a channel of constant depth $\overline{d}$, connected to a planely sloping beach of angle β. A sketch (distorted scale) of this canonical beach is displayed in Fig. 1. Here, $\overline{H}$ is the physical incident wave height, which has been normalized with respect to $\overline{d}$ to define the nondimensional wave height H. More than 40 experiments involving solitary waves of varying heights were performed Synolakis (1986). The height-to-depth ratio $H = \overline{H}/\overline{d}$ ranged from 0.021 to 0.626. The water level profiles at several nondimensional times ($t = \overline{t}\sqrt{\overline{g}/\overline{d}}$, where $\overline{t}$ and $\overline{g}$ are the physical time and gravity accerelation), were measured for waves with $H = 0.0185$, $H = 0.045$, and $H = 0.3$. Howeve,r in this paper only the $H = 0.0185$ and $H = 0.3$ wave experiments are shown and compared to results of the numerical models. According to observations, the solitary wave breaking occurs when $H > 0.045$. Therefore, the experimental wave with $H = 0.0185$ did not break, thus, simulating a more realistic tsunami. The choice for $\overline{d}$ in this laboratory experiment is somewhat arbitrary, but the depth used was approximately 0.3 m.

The comparison of results of various models for the BP4 is performed by comparing numerically computed water surface profiles to the laboratory data at certain given times for the nonbreaking case ($H = 0.0185$), then, by doing the same for the more challenging breaking waves case, $H = 0.3$. Readers interested in reproducing numerically BP4 can find the required information at https://github.com/rjleveque/nthmp-benchmark-problems.

3.2. Laboratory Experiment: Solitary Wave on a Conical Island

To validate and compare numerical models for a case including more complex wave propagation and run-up, Synolakis *et al.* (2007) proposed a 3-D laboratory experiment that mimics the inundation inflicted on Babi Island by the tsunami of December 12th, 1992, Flores, Indonesia Yeh *et al.* (1994). This particular tsunami struck the circular shaped island from the north, but caused unexpected high inundation in the southern or opposite side of the island. A model of the circular island was constructed in the

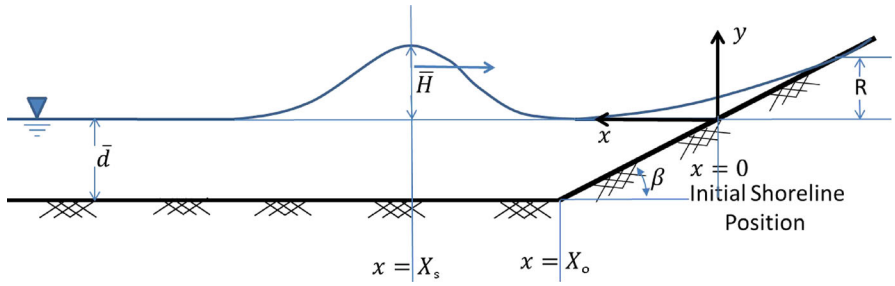

Figure 1
Schematic of the laboratory experiment setup for BP4 and definition of parameters for the canonical bathymetry, i.e., sloping beach connected to a constant depth region

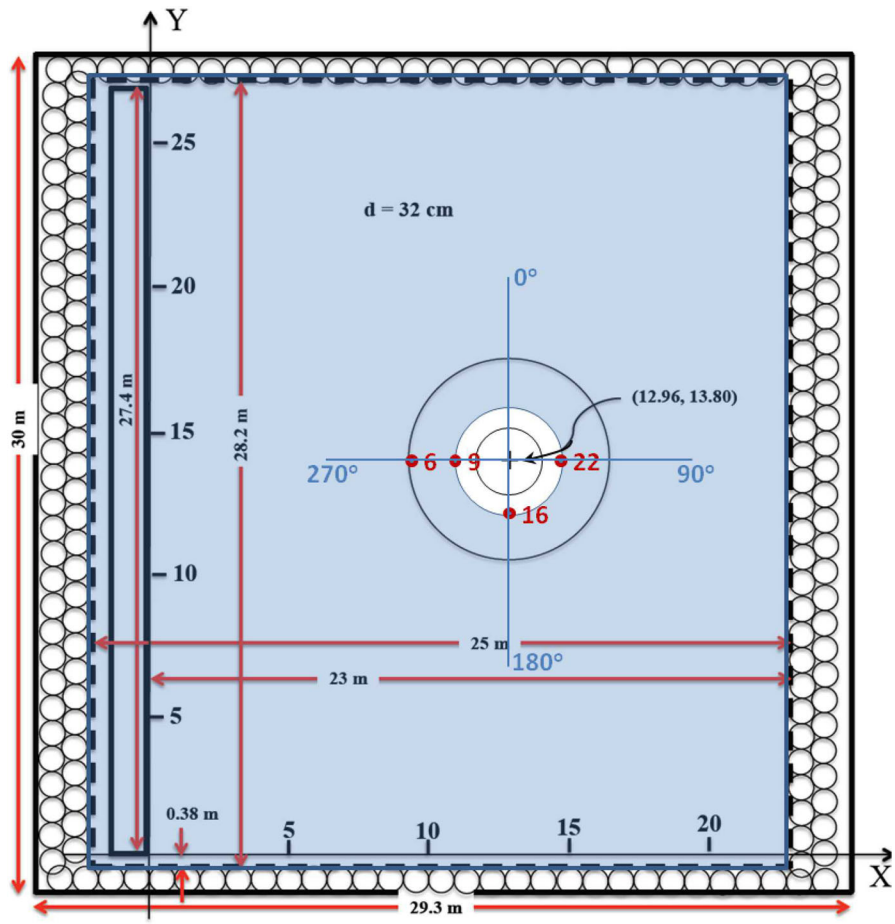

Figure 2
Schematic layout of the laboratory experiment setup for BP6 showing the basin configuration, coordinate system, and location of gauges. *Solid lines* represent basin walls and wavemaker surfaces. *Circle* along walls and *dashed lines* represent wave absorbing material. Note the gaps of approximately 0.38 m between each end of the wavemaker and the adjacent wall (figure courtesy of Frank Gonzalez)

large-scale wave tank of the US Army Engineer Waterways Experiment Station, Vicksburg, Mississippi (Briggs *et al.* 1995; Liu *et al.* 1995), to understand the cause of observed high inundation at the opposite side of the island. The lab experiment is further depicted and updated in the workshop

proceedings NTHMP (2012), in which it is referred to as BP6.

Figure 2 shows a sketch of the laboratory experiment setup. It should be noted that additional details of the basin configuration and physical conditions were incorporated into the numerical models to more accurately reproduce the original physical conditions of the experiments. This information was obtained directly from Dr. M. Briggs, in collaboration with Dr. F. Gonzalez. The basin had dimensions of 29.3 × 30 m. A wave-absorbing material was installed around the walls of the basin, reducing its dimension to 25 × 28.2 m. The wave-absorbing material was a pad of synthetic horsehair, 2 inches thick, rolled into cylinders of approximately 0.9 m diameter, characterized by a reflection coefficient that varied somewhat with wave frequency but oscillated around 12 %. The effective length of the wavemaker was 27.4 m. The differences between this more accurate wave basin setup (Fig. 2) from the previously published basin setup stem primarily from the fact that: (a) the wavemaker face extended about 2 m into the wave basin and (b) a gap of approximately 0.38 m exists in-between each end of the wavemaker and the lateral wall. The island had the shape of a truncated circular cone with diameters of 7.2 m at the toe and 2.2 m at the crest (conical island). The total vertical height of the island was approximately 0.625 m, with a horizontal to vertical slope ratio of 4:1, i.e., $\beta = 14^{\circ}$. The water depth was set at 0.32 m in the basin. The interested reader is referred to http://chl.erdc.usace.army.mil/chl.aspx?p=s&a=Projects;35 or http://nctr.pmel.noaa.gov/benchmark/Laboratory/Laboratory_ConicalIsland/index.html for more detailed descriptions of laboratory experiments and data files. The required information that is needed to reproduce numerically this BP can be found at https://github.com/rjleveque/nthmp-benchmark-problems. One of the challenges in numerically modeling this experiment is to accurately simulate the incident wave refraction around the island (edge waves), the amplification of the incident wave at the opposite side of the island, and the run-up associated with the edge wave around the island.

It is important to mention that the above BP's results were not concealed to the modelers (open experiment results) because the difficult nature of reproducing accurately these lab experiments. Modelers were allowed to adjust efficiently their numerical model parameters (e.g., space-time resolution, friction, etc.) to ensure best matching result against the BP's results. However, modelers were blinded with respect to other modeler's results. The model comparison is intended to confirm sources or expected sources of variability among the different approaches used on the O&I tsunami numerical models.

4. *Performance of Numerical Models*

As it is indicated in Synolakis *et al.* (2007) and NTHMP (2012), maximum allowable error thresholds are used to decide whether a model has adequately simulated the designated BP. Specifically, for BPs in the laboratory experiment category, a 10 % or less average relative error on model parameters with respect to the reference data is suggested to be achieved. If a laboratory experiment features breaking waves, then a 20 % or less average relative error is allowed.

In the following, the performance of the eight O&I models applied as part of the workshop is illustrated through a cross-comparison for BP4, based on laboratory experiments for a solitary wave running up a 1:19.85 plane beach (so-called "Single wave on a simple beach"). Figure 3 shows five snapshots of surface elevation computed at various nondimensional times $t = 30$ to 70 by $\delta t = 10$ increments, versus the experimental reference data, for an initial nondimensional solitary wave of height $H = 0.0185$. Overall, we see a good agreement between the numerical solutions and the laboratory measurements for all selected times, corresponding to both the propagation/shoaling and run-up of the wave. It should be noted that differences among numerical solutions are smaller than differences between any of the model solutions and the laboratory data. At $t = 50$, which is near the maximum run-up ($t = 55$), two models based on the hydrostatic-NSWEs (ALASKA and GeoClaw) predict a slightly higher run-up than the other models and the experimental data. These differences could be attributed in part to the zero friction assumption and fine spatial discretization used in their numerical solution.

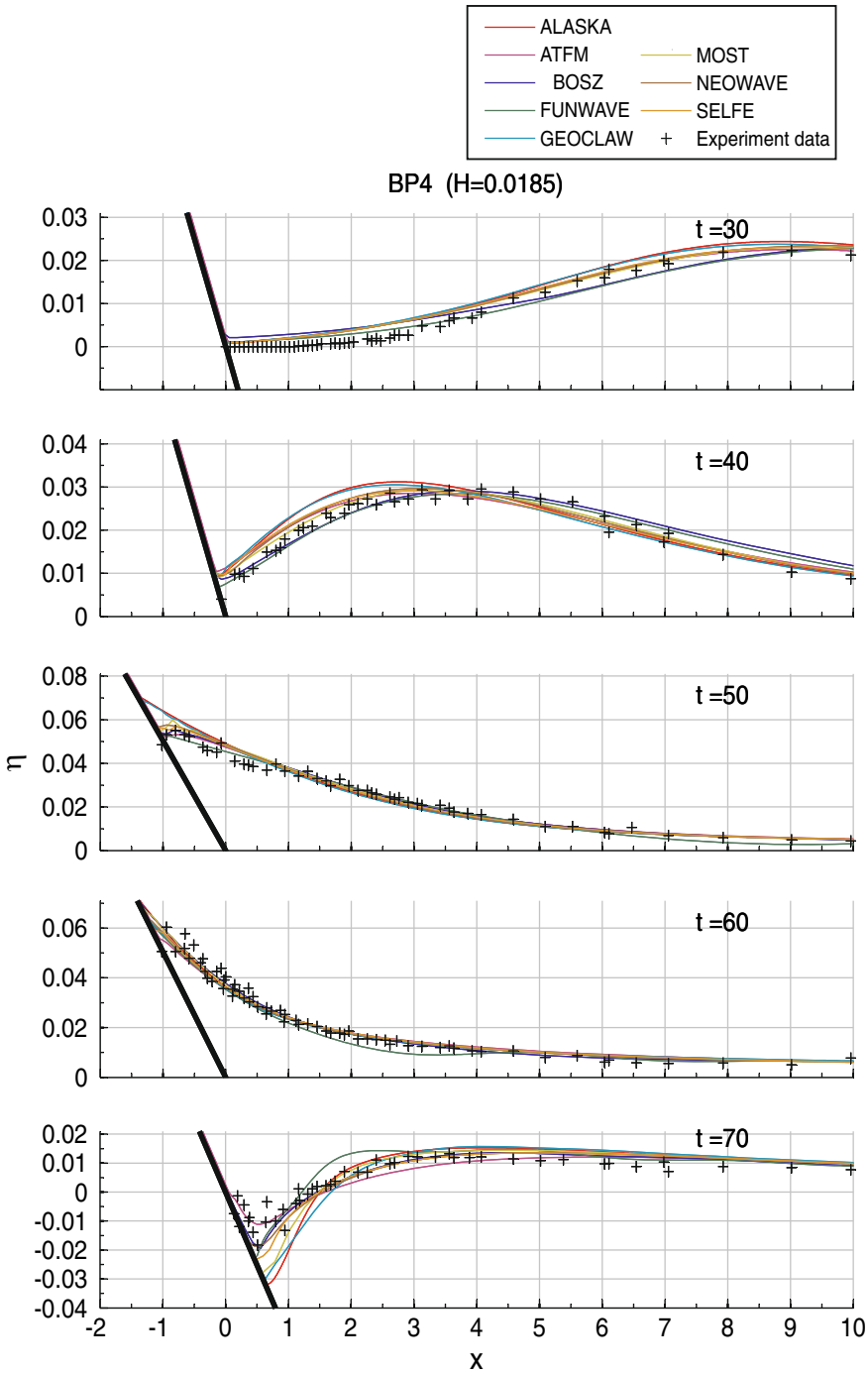

Figure 3
Water surface snapshots comparison of experimental data (*crosses*) versus model results (*colored solid lines*) during run-up of a nonbreaking solitary wave ($H = 0.0185$) over a 1:19.85 slope at $t = [30, 40, 50, 60, 70]$

However, other models, e.g., MOST and ATFM, captured the run-up somewhat better. In the case of ATFM, the improvement is likely due to the addition of the nonhydrostatic component (dispersive terms) to account for dispersive wave propagation. Similarly, the MOST model mimics this effect without the

explicit use of dispersive terms in the governing equations, by exploiting the numerical dispersion inherent to its finite-difference numerical scheme. It is also noticeable in Fig. 3 that models that include dispersive effects produce results better at $t = 50$ and 60 than nondispersive models. The numerical solutions vary the most at $t = 70$, which corresponds to the maximum rundown. There, we see that the nondispersive models (MOST, ALASKA and GEOCLAW) compute larger rundowns than the dispersive models (ATFM, BOSZ, FUNWAVE and NEOWAVE). It is important to mention that the approach of tuning numerical dispersion to match physical dispersion is most appropiately applied in the linear wave propagation regime (deep water), but it is still unclear how well the linear dispersion approximation works when the waves become nonlinear. In this particular BP, SELFE has been configured for the 2-D hydrostatic (nondispersive) mode, from its multiple possibilities, for maximum efficiency. Nevertheless, SELFE results are quite good and comparable to the dispersive models. This is due to the use of a finer unstructured grid in the horizontal dimension, close to the coastline or run-up region. For maximum wave amplitude or run-up of the surface elevation computed at various nondimensional times ($t = [30, 40, 50, 60, 70]$), regardless of the location, the mean models' errors range between 2 % and 10 %.

Figure 4 similarly presents a cross-comparison for the BP4 case $H = 0.30$ of the surface elevation computed at various nondimensional times $t = 15$ and 30 by $\delta t = 5$ increments, computed by four models, as compared to laboratory experiments. This is a very challenging case in which the wave breaks during run-up in the laboratory experiments. Only the results of models that feature the dispersive effects (e.g., explicit dispersive terms in the governing equations) are presented in the model cross-comparison (ATMF, BOSZ, FUNWAVE, and NEOWAVE). Results show that the inclusion of dispersive effects in the models' scheme allows the wave to initially steepen without breaking, between $t = 15$ and $t = 20$, which results in a good match with laboratory measurements. During this time period, a slight shift of the surface elevation is noticeable on models than reproduce better the wave amplitude (NEOWAVE and ATFM). This condition is mainly attributed to the amplitude dispersion effects, that make higher waves travel slightly faster, and probably to some extent, to the advection scheme, e.g., the VOF approach used for flow advection in the ATFM model, and the momentum-conserved advection and upwind flux approximation used in NEOWAVE. For maximum wave amplitude or run-up obtained from the surface elevation computed at various nondimensional times ($t = [15, 20, 25, 30]$), regardless of the location, the mean models' errors range between 5 % and 12 %. These errors have a moderate variation amongst models and are below the 20 % threshold recommended by the OAR-PMEL-135 report for laboratory experiments that feature breaking waves.

For NSWE (nondispersive) models, case $H = 0.30$ of BP4 becomes even more challenging (the results are not presented in this paper). The existence of strong wave breaking does prevent a good agreement of the NSWE solutions with laboratory measurements (for details on NSWE solutions see each individual model reports in NTHMP (2012). For instance, nondispersive models predict that the leading front of the solitary wave will steepen and become singular shortly after the initiation of the computations. The numerical singularity propagates towards the beach until it meets the shoreline where the singularity dissipates. Since the numerical dispersion can compensate for the absence of physical dispersion in nondispersive models (e.g., by adjusting the spatial discretization as the MOST model does) a better agreement with the reference data is possible. This topic is still an active area of research in NSWE models.

In BP6, experiments with different incident wave heights were conducted in the large-scale wave tank at Coastal Engineering Research Center, Vicksburg, Mississippi. The time series of surface elevation comparison and associated errors at gauges 6, 9, 16, and 22 (Fig. 2) for a variety of incident solitary waves impinging onto a conical island are shown in Fig. 5. The case $H = 0.181$, which is a breaking wave, is selected from the subset of laboratory experiment to validate the models' wave height. For the run-up cross-comparison, three different wave heights or cases are selected from the laboratory experiment, i.e., cases $H = 0.045$, $H = 0.096$ and $H = 0.181$. The snapshot times have been selected to avoid the first reflection of the incident

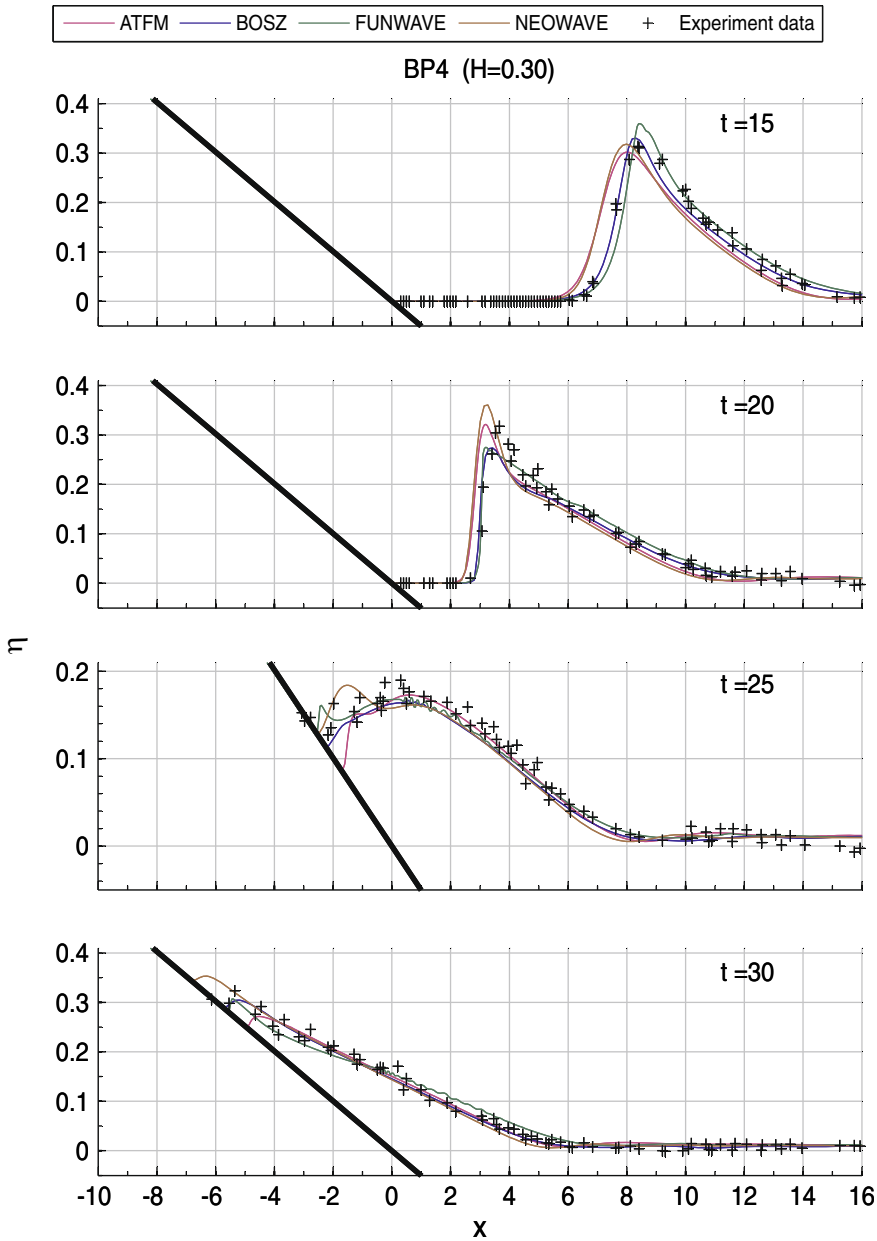

Figure 4
Water surface snapshots comparison of experimental data (*crosses*) versus model results (*colored solid lines*) during run-up of a breaking solitary wave ($H = 0.30$) over a 1:19.85 slope at $t = [15, 20, 25, 30]$

wave. For all hydrostatic NSWE models, such as ALASKA, GEOCLAW, and MOST, the simulated waves are seen to steepen faster than in laboratory experiments. This is a well-known effect of the shallow water approximation, where the lack of dispersive terms yields so-called "shallow water steepening" of waves. Again, visual examination of the models' results reveals that the dispersive models, such as ATFM, BOSZ, FUNWAVE, NEOWAVE, and SELFE, capture the water level dynamics slightly better than the nondispersive models. However, while dispersive models based on the Boussinesq-type or nonhydrostatic approximations feature the dispersive effects, there is no appreciable improvement over the

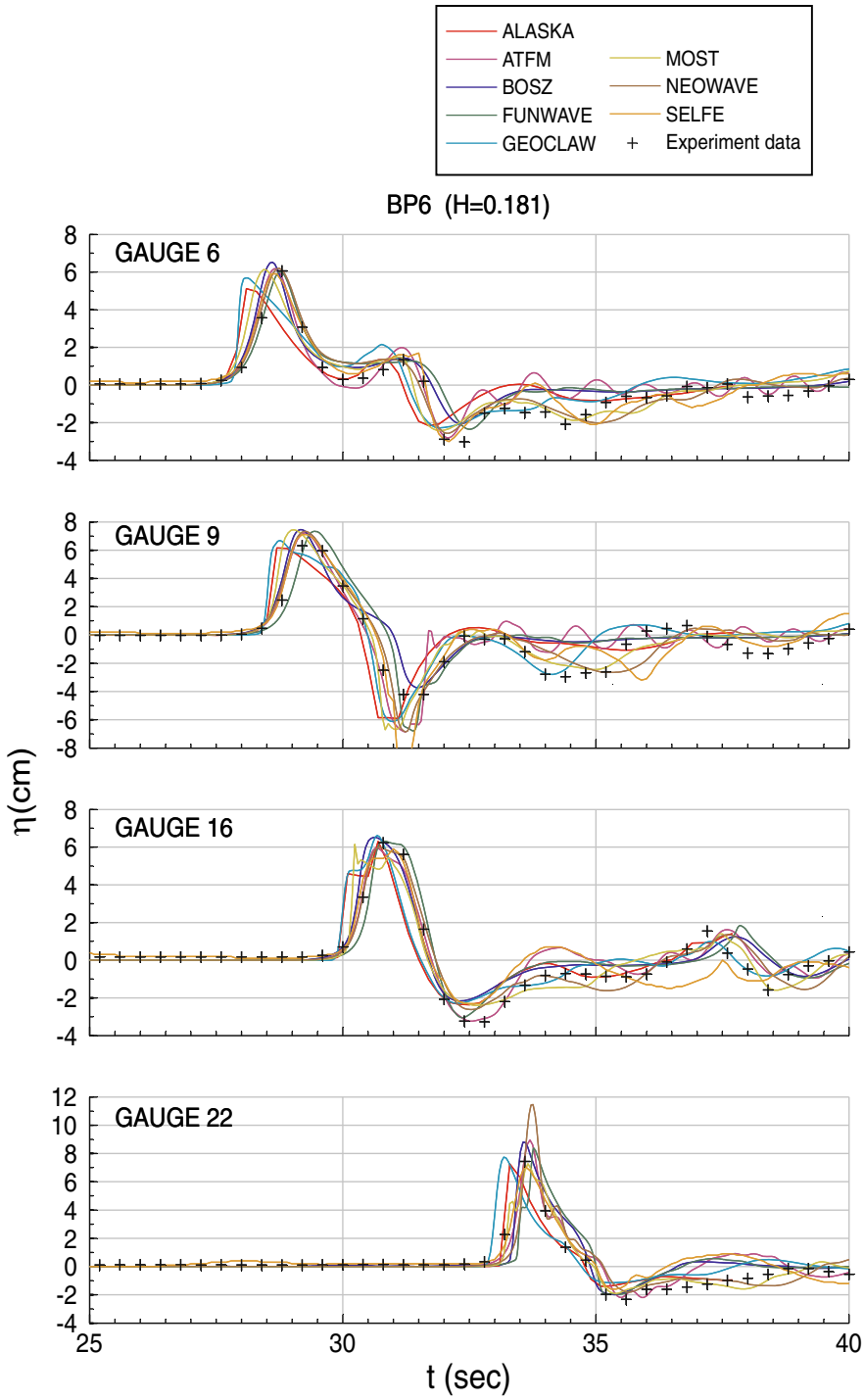

Figure 5
Water surface time series comparison between experimental data (*crosses*) versus model results (*colored solid lines*) of a solitary wave of $H = 0.30$ at gauges shown in Fig. 2

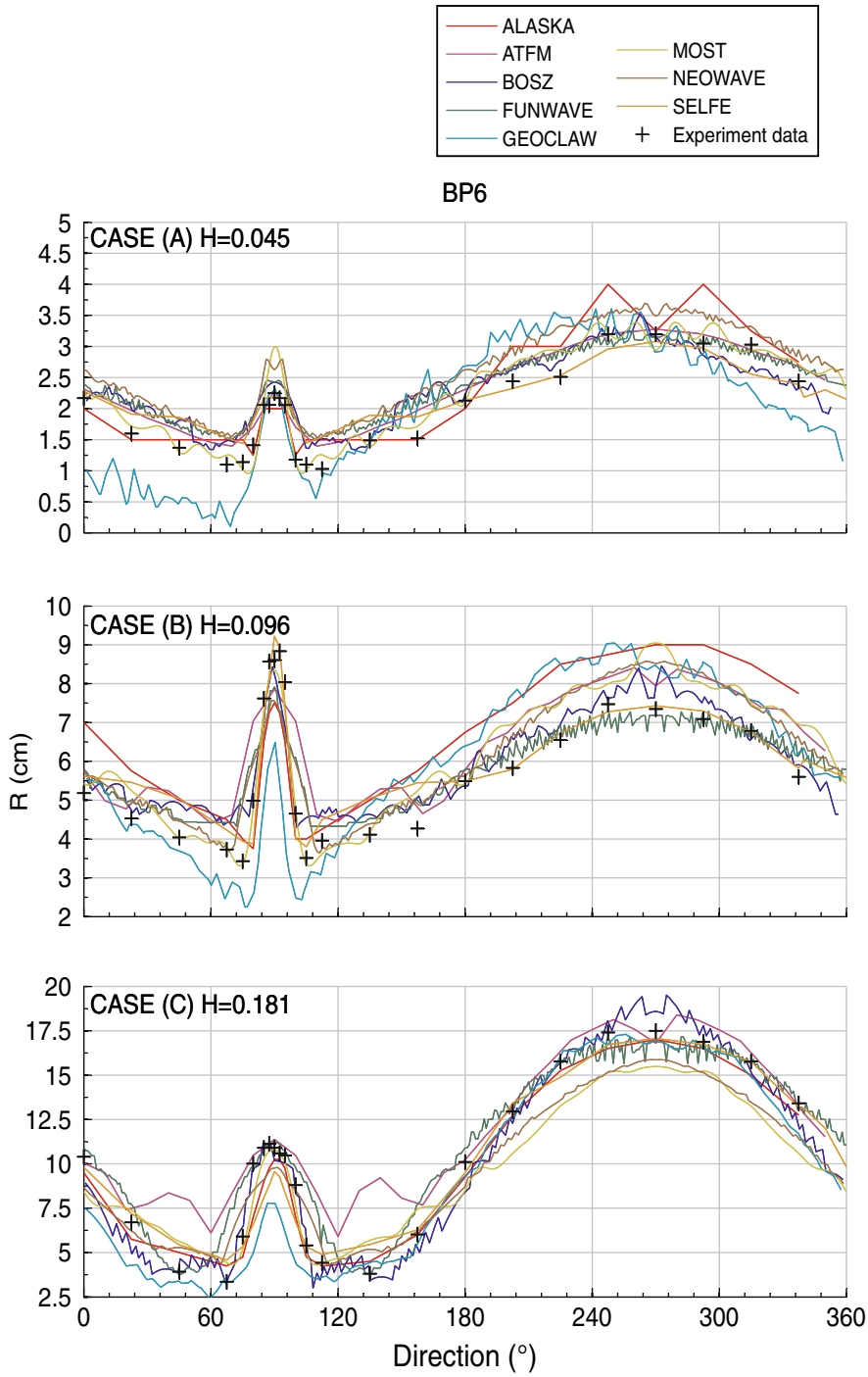

Figure 6
Run-up comparison around a conical island between experimental data (*crosses*) versus model results (*colored solid lines*) for $H = [0.045, 0.096, 0.181]$

hydrostatic NSWE models in matching this particular set of laboratory observations. For maximum wave amplitude at gauges, regardless of the location the maxima occurred, the mean model errors range between 6 % and 12 %. These model errors have a moderate variation, and there is a clear trend that dispersive models perform slightly better. All model errors for BP6 case $H = 0.181$ are below the 20 % threshold recommended in OAR-PMEL-135.

One of the challenges in modeling the observed wave is the application of appropriate boundary conditions and the generation of waves in the numerical models. Although various techniques were employed to address these challenges, all computed solutions matched well the observed water level dynamics at the given locations or gauges.

Figure 6 shows the modeled maximum run-up distribution versus laboratory experiments, around the conical island, for all three wave height cases ($H = [0.045, 0.096, 0.181]$). Here again it is observed that, in general, dispersive models reproduce the maximum run-up slightly better. The noticeable small asymmetry that is seen in the model run-up results is believed to be due to misalignment between the adopted grid for the basin and the axis of the conical island. The models' runup mean relative errors, range between 3 % and 10 %. As they do not differ by more than 10 % from the laboratory measurements, maximum run-up values predicted by all models are considered to be fairly good.

5. Conclusions

Results of the systematic model validation and cross-comparison exposed some of the limitations and clearly identified key attributes of the operational and inundation-based (O&I) tsunami models. The analysis of validation results for each model, regardless of the selected BPs, and the model cross-comparison, show that all the presented models are deemed adequate for predicting the propagation and run-up of tsunami waves in the geophysical conditions covered by the applicable BPs (category of experiment). Hence, these models are also deemed acceptable for the ongoing inundation mapping activity under NTHMP.

More specifically, in BP4, for case $H = 0.0185$, the maximum wave amplitude model errors were below 10 % (ranging between 2 % and 10 %). For $H = 0.30$, the breaking wave case, the maximum wave amplitude model errors ranged between 5 % and 12 %. This is below the accepted standard error for laboratory experiments BPs featuring breaking waves (20 %). Results show that the inclusion of wave dispersion effects in the numerical models (as compared to the NSWEs models) allows the wave to initially steepen without breaking at an early stage of wave shoaling (between $t = 15$ and 20), yielding results in a good agreement with laboratory measurements.

In BP6, for the case $H = 0.181$, a breaking wave, a clear trend was observed showing that dispersive models perform slightly better than nondispersive models. Model errors are kept below the 20 % threshold recommended in OAR-PMEL-135.

Results presented in this paper represent an important step in attaining consistency in tsunami inundation modeling among federal agencies, states, and communities. As it is recognized by the tsunami research community, the validation of numerical models is a continuous process. Even proven numerical models must be subjected to additional testing as new knowledge/methods or better data are obtained. New BPs must, thus, continuously be defined to address new tsunami source characteristics or complex coastal impact. In light of this, all O&I tsunami numerical models should regularly be tested against an evolving set of relevant BPs, for continuous validation and verification. While most of the OAR-PMEL-135 BPs had been developed for validating and verifying model simulations for coseismic tsunami sources, few had been developed for landslide sources. Tsunami modelers in general agree that some new and perhaps more relevant BPs, particularly for the latter sources (landslide), should be proposed. Additionally, some of the models, which are based on Boussinesq, nonhydrostatic, or NS equations featured more extended physics than analytic BPs in the original OAR-PMEL-135 set, which were based on SWE or NSWE and, thus, do not feature dispersion; hence, the comparison of model results with such solutions (analytical) should be made with this caveat in mind.

Acknowledgments

The authors wish to thank the NTHMP and the National Oceanic and Atmospheric Administration (NOAA) for providing funding for the activities associated with this work at the Texas A&M at Galveston workshop. We acknowledge the individual contributions of the workshop participants (see list below); this paper reflects a minuscule part of substantial work incurred by the participants to validate the models. This paper has greatly benefited from the research sponsored by the Cooperative Institute For Alaska Research (CIFAR), NOAA, under cooperative agreement NA08OAR4320751 with the University of Alaska. Additionally, we thank all reviewers that provided invaluable discussion and suggestions. Workshop participants and contributors are: Stéphane Abadie, Frank González, Bill Knight, Fengyan Shi, Elena Tolkova, Yoshiki Yamazaki, Loren Pahlke, Amanda Wood, Gyeong-Bo Kim, Marie Eble and Rick Wilson.

References

Abadie, S. D., Harris, J. C., Grilli, S. T., and Fabre, R. (2012). "*Numerical modeling of tsunami waves generated by the flank collapse of the Cumbre Vieja Volcano (La Palma, Canary Islands) : Tsunami source and near field effects*". J. Geophys. Res., *117*, C05030.

Abadie, S. D., Morichon, S. D., Grilli, S., and Glockner, S. (2010). "*Numerical simulation of waves generated by landslides using a multiple-fluid Navier–Stokes model*". Coastal Engineering, *57*(9), 779–794.

Arakawa, A. and Lamb, V. (1977). "Computational design of the basic dynamical processes of the UCLA general circulation model". Methods in Computational Physics, 17 Academic Press, 174–267.

Berger, M. J. and LeVeque, R. J. (1998). "*Adaptive mesh refinement using wave-propagation algorithms for hyperbolic systems*". SIAM J. Numer. Anal., *35*, 2298–2316.

Briggs, M. J., Synolakis, C. E., Harkins, G. S., and Green, D. (1995). "*Laboratory experiments of tsunami runup on a circular island*". Pure Appl. Geophys., *144*, 569–593.

Burwell D, Tolkova E, Chawla A. (2007). "*Diffusion and dispersion characterization of a numerical tsunami model*". Ocean Modelling, *19*(1–2), 10–30.

Dunbar, P. K. and Weaver, C. S. (2008). "U.S. states and territories national tsunami hazard assessment: Historic record and sources for waves". Report No. Report to National Tsunami Hazard Mitigation Program, NGDC, USGS.

Fischer, G. (1959). "*Ein numerisches verfahren zur errechnung von windstau und gezeiten in randmeeren*". Tellus, *11*, 60–76.

Goring, D. G. (1978). "Tsunamis-the propagation of long waves onto a shelf". Report No. KH-R-38, WM. Keck Laboratory of Hydraulics and Water Resources, California Institute of Technology.

Grilli, S. T., Dias, F., Guyenne, P., Fochesato, C., and Enet, F. (2010). "Progress in fully nonlinear potential flow modeling of 3D extreme ocean waves". Advances in Numerical Simulation of Nonlinear Water Waves (Series in Advances in Coastal and Ocean Engineering, Vol. 11, ISBN: 978-981-283-649-6), Word Scientific Publishing Co., 55.

Grilli, S. T., Harris, J., Shi, F., Kirby, J. T., Bakhsh, T. T., Estibals, E., and Tehranirad, B. (2013). "Numerical modeling of coastal tsunami dissipation and impact". In Proc. 33rd Intl. Coastal Engng. Conf., J. Mc Kee Smith, ed., (ICCE12, Santander, Spain, July, 2012), Word Scientific Publishing Co., Pte. Ltd., 12 pps. (in press).

Grilli, S. T., Harris, J. C., Tajalibakhsh, T., Masterlark, T. L., Kyriakopoulos, C., Kirby, J. T., and Shi, F. (2012). "Numerical simulation of the 2011 Tohoku tsunami based on a new transient FEM co-seismic source: Comparison to far- and near-field observations". Pure and Applied Geophysics, 27 pps. doi:10.1007/s00024-012-0528-y (published online).

Hammack, J. L. (1972). "Tsunamis-A model for their generation and propagation". Report No. KH-R-28, LWM. Keck Laboratory of Hydraulics and Water Resources, California Institute of Technology.

Hansen, W. (1956). "*Theorie zur errechnung des wasserstands und derstromungen in randemeeren*". Tellus, *8*, 287–300.

Harlow, F. H. and Welch, J. E. (1965). "*Numerical calculation of time-dependent viscous incompressible flow of fluid with a free surface*". The Physics of Fluids, *8*, 2182–2189.

Harris, J. C., Grilli, S. T., Abadie, S. D., and Tajalibakhsh, T. (2012). "Near- and far-field tsunami hazard from the potential flank collapse of the Cumbre Vieja Volcano". Proc. 22nd Offshore and Polar Engng. Conf., I. S. ofOffshore and P. Engng., eds., (ISOPE12, Rodos, Greece, June 17–22, 2012), 242–249.

Hirt, C. W. and Nichols, B. D. (1981). "*Volume of fluid method for the dynamics of free boundaries*". J. Comp. Phys., *39*, 201–225.

Horrillo, J. J., Wood, A. L., Williams, C., Parambath, A., and Kim, G.-B. (2010). "Construction of tsunami inundation maps in the Gulf of Mexico". Report Award Number: NA09NWS4670006, National Tsunami Hazard Mitigation Program (NTHMP), National Weather Service Program Office, NOAA.

Horrillo, J., A. Wood, G.-B Kim, and A. Parambath. (2013). "A simplified 3-D Navier–Stokes numerical model for landslide-tsunami: Application to the Gulf of Mexico". J. Geophys. Res. Oceans, *118*, 6934–6950, doi:10.1002/2012JC008689.

Imamura, F. (1996). "Review of tsunami simulation with a finite difference method". Long-Wave Runup Models, H. Yeh, P. Liu, and C. Synolakis, eds., Word Scientific Publishing Co., 25–42.

Imamura, F., Goto, C., Ogawa, Y., and Shuto, N. (1995). Numerical Method of Tsunami Simulation with the Leap-Frog Scheme. IUGG/IOC Time Project Manuals (May).

Ioualalen, M., Asavanant, J., Kaewbanjak, N., Grilli, S. T., Kirby, J. T., and Watts, P. (2007). "*Modeling the 26 December 2004 Indian Ocean tsunami: Case study of impact in Thailand*". J. of Geophys. Res., *112*, C07024.

Kirby, J. T., Wei, G., Chen, Q., Kennedy, A. B., and Dalrymple, R. A. (1998). "FUNWAVE1.0: Fully nonlinear Boussinesq wave model documentation and user's manual". Report No. NO. CACR-98-06, University of Delaware.

Kowalik, Z., Knight, W., Logan, T., and Whitmore, P. (2005). "*Numerical modeling of the global tsunami: Indonesian tsunami*

of 26 December 2004". Science of Tsunami Hazards, *23*(1), 40–56.

Kowalik, Z. and Murty, T. S. (1993). Numerical Modeling of Ocean Dynamics. World Scientific, 481 pp.

Kowalik, Z. and Whitmore, P. M. (1991). "*An investigation of two tsunamis recorded at Adak, Alaska*". Science of Tsunami Hazards, *9*, 67–83.

Liu, P. L.-F., Cho, Y.-S., Briggs, M. J., Kanoglu, U., and Synolakis, C. E. (1995). "*Runup of solitary wave on circular island*". Journal of Fluid Mechanics, *302*, 259–285.

Lynett, P., Wu, T.-R., and Liu, P. L.-F. (2002). "*Modeling wave runup with depth-integrated equations*". Coastal Engineering, *46*(2), 89–107.

Ma, G., Shi, F., and Kirby, J. T. (2012). "*Shock-capturing non-hydrostatic model for fully dispersive surface wave processes*". Ocean Modelling, (43–44), 22–35.

Nichols, B. D. and Hirt, C. W.(1975). "Method for calculating multi-dimensional, transient free surface flow past bodies". Proc. of the 1st Int. Conf. Num. Ship Hydrodynamics, Gaithersburg, Maryland, US., 253–277.

Nichols, B. D., Hirt, C. W., and Hotchkiss, R. S. (1980). "SOLA-VOF: A solution algorithm for transient fluid flow with multiple free boundaries". Report No. LA-8355, Los Alamos National Laboratory.

Nicolsky, D., Suleimani, E., and Hansen, R. (2011). "*Validation and verification of a numerical model for tsunami propagation and runup*". Pure and Applied Geophysics, *168*(6–7), 1199–1222.

NTHMP (2012). "National Tsunami Hazard Mitigation Program. Proceedings and Results of the 2011 NTHMP Model Benchmarking Workshop". NOAA-NTHMP, Boulder: U.S. Department of Commerce/NOAA/NTHMP; (NOAA Special Report), 436 pp.

Nwogu, O. (1993). "*An alternative form of the Boussinesq equations for nearshore wave propagation*". J. Waterway, Port, Coastal, and Ocean Engineering, *119*, 618–638.

Peregrine, D. (1967). "*Long waves on a beach*". Journal of Fluid Mechanics, *27*(4), 815–827.

Rider, J. and Kothe, D. B. (1995). "Stretching and tearing interface tracking methods". 12th AIAA Comp. Fluid Dynamics Conference, Jun. 20, 1995, San Diego. Paper Number AIAA-95-1717 or LA-UR-95-1145.

Roeber, V. and Cheung, K. F. (2012). "*Boussinesq-type model for energetic breaking waves in fringing reef enviroments*". Coastal Engineering, (70), 1–20.

Shi, F., Kirby, J. T., Harris, J. C., Geiman, J. D., and Grilli, S. T. (2012). "A high-order adaptive time-stepping TVD solver for boussinesq modeling of breaking waves and coastal inundation". Ocean Modeling, *43–44*, 36–51.

Stelling, G. S. and Zijlema, M. (2003). "*An accurate and efficient finite-difference algorithm for nonhydrostatic free-surface flow with application to wave propagation*". International Journal for Numerical Methods in Fluids, *43*(1), 1–23.

Synolakis, C. E. (1986). "The runup of long waves". Ph.D. thesis, California Institute of Technology, Pasadena, California, 91125, 228 pp.

Synolakis, C. E., Bernard, E. N., Titov, V. V., Kanoglu, U., and González, F. I. (2007). "OAR PMEL-135 standards, criteria, and procedures for NOAA evaluation of tsunami numerical models". Report No. NOAA Tech. Memo. OAR PMEL-135, NOAA/Pacific Marine Environmental Laboratory, Seattle, WA.

Synolakis, C. E., Bernard, E. N., Titov, V. V., Kanoglu, U., and González, F. I. (2008). "*Validation and verification of tsunami numerical models*". Pure Appl. Geophys., *165*, 2197–2228. doi:10.1007/s00024-004-0427-y.

Tang, L., Titov, V.V., Bernard, E., Wei, Y., Chamberlin, C., Newman, J.C., Mofjeld, H., Arcas, D., Eble, M., Moore, C., Uslu, B., Pells, C., Spillane, M.C., Wright, L.M., and Gica, E. (2012). "*Direct energy estimation of the 2011 Japan tsunami using deep-ocean pressure measurements*". J. Geophys. Res., doi:10.1029/2011JC007635.

Tappin, D. R., watts, P., and Grilli, S. T. (2008). "*The Papua New Guinea Tsunami of 17 July 1998: Anatomy of a catastrophic event*". Nat. Hazards Earth Syst. Sci., *8*, 243–266.

Titov, V. and Synolakis, C. E. (1995). "*Evolution and runup of breaking and nonbreaking waves using VTSC2*". Journal of Waterway, Port, Coastal and Ocean Engineering, *126*(6), 308–316.

van Leer, B. (1977). "*Towards the ultimate conservative difference scheme III. Upstream-centered finite-difference schemes for ideal compressible flow*". J. Comp. Phys., *23*(3), 263–275.

Watts, P., Grilli, S. T., Kirby, J. T., Fryer, G. J., and Tappin, D. R. (2003). "*Landslide tsunami case studies using a Boussinesq model and a fully nonlinear tsunami generation model*". Natural Hazards and Earth System Sciences, (3), 391–402.

Wei, G., Kirby, J. T., Grilli, S. T., and Subramanya, R. (1995). "*A fully nonlinear Boussinesq model for free surface waves. Part 1: Highly nonlinear unsteady waves*". J Fluid Mech, *294*, 71–92.

Wei, Y., Bernard, E., Tang, L., Weiss, R., Titov, V., Moore, C., Spillane, M., Hopkins, M., and Kanoglu, U. (2008). "*Real-time experimental forecast of the Peruvian tsunami of August 2007 for U.S. coastlines*". Geophysical Research Letters, *35*, L04609.

Whitmore, P. M. and Sokolowski, T. J. (1996). "*Predicting tsunami amplitudes along the North American coast from tsunamis generated in the northwest Pacific Ocean during tsunami warnings*". Science of Tsunami Hazards, *14*, 147–166.

Yamazaki, Y., Cheung, K. F., and Kowalik, Z. (2011a). "*Depth-integrated, non-hydrostatic model with grid nesting for tsunami generation, propagation, and run-up*". J. Numer. Meth. Fluids, *67*, 2081–2107.

Yamazaki, Y., Kowalik, Z., and Cheung, K. F. (2009). "*Depth-integrated, non-hydrostatic model for wave breaking and run-up*". Int. J. Numer. Meth. Fluids, *61*(5), 473–497.

Yamazaki, Y., Lay, T., Cheung, K. F., Yue, H., and Kanamori, H. (2011b). "*Modeling near-field tsunami observations to improve finite-fault slip models for the 11 March 2011 Tohoku earthquake*". Geophys. Res. Lett., *38*, L00G15, doi:10.1029/2011GL049130.

Yeh, H., Liu, P.-F., Briggs, M., and Synolakis, C. E. (1994). "*Tsunami catastrophe in Babi Island*". Nature, *372*, 6503–6508.

Zhang, Y. and Baptista, A. M. (2008). "*An efficient and robust tsunami model on unstructured grids*". Pure and Applied Geophysics, *165*, 2229–2248.

(Received March 4, 2014, revised June 20, 2014, accepted June 26, 2014)